Potential climate warming effects on ice covers of small lakes in the contiguous U.S.

Xing Fang [a,1], Heinz G. Stefan [b,*]

[a] *Lamar University, Department of Civil Engineering, Beaumont, TX 77710, USA*
[b] *University of Minnesota, Department of Civil Engineering, Minneapolis, MN 55414, USA*

Abstract

To simulate effects of projected climate change on ice covers of small lakes in the northern contiguous U.S., a process-based simulation model is applied. This winter ice/snow cover model is associated with a deterministic, one-dimensional year-round water temperature model. The lake parameters required as model input are surface area, maximum depth, and Secchi depth as a measure of radiation attenuation. The model is driven by daily weather data. Weather records from 209 stations in the contiguous U.S. for the period 1961–1979 were used to represent past climate conditions. The projected climate changes due to a doubling of atmospheric CO_2 were obtained from the output of the Canadian Climate Center Global Circulation Model. To illustrate the effect of projected climate change we present herein winter ice cover characteristics simulated, respectively, with inputs of past climate conditions (1961–1979), with inputs of a projected $2 \times CO_2$ climate scenario as well as differences of those values. The dependence of ice cover characteristics on latitude and lake characteristics has been quantified by making simulations for 27 lake types at 209 locations across the contiguous U.S. It was found that the $2 \times CO_2$ climate scenario is projected to delay ice formation on lakes by as much as 40 days and melt ice by up to 67 days earlier. Maximum ice thicknesses are projected to be reduced by up to 0.44 m (Sault Ste. Marie, MI), and the ice cover periods will be shorter by up to 89 days (Rock Springs, WY). The largest changes are projected to occur east of Idaho from the Canadian border down to the states of Colorado, Nebraska, and Iowa and the northern parts of Illinois, Indiana, Ohio, and Pennsylvania. These changes would reduce fish winterkill in most shallow lakes of the northern states of the contiguous U.S. but may endanger snowmobiles and ice fishermen. © 1998 Elsevier Science B.V. All rights reserved.

1. Introduction

Ice covers on lakes form in response to meteorological conditions. Ice formation is usually associated with the coldest water temperature in a lake, calm wind conditions and low air temperatures. Ice melt is related to significant solar radiation absorption and above freezing air temperatures (Ashton, 1986). Fish winterkill can occur in shallow eutrophic lakes near the end of an extended ice cover period when dissolved oxygen concentrations in the water drop below 2 mg/l. Low dissolved oxygen concentrations in ice-covered lakes are caused by suppres-

---

* Corresponding author. Tel.: +1-612-627-4585; +1-612-625-2810; fax: +1-612-627-4690; e-mail: stefa001@tc.umn.edu.

[1] Tel.: +1-409-880-2287; fax: +1-409-880-8121; e-mail: fangxu@hal.lamar.edu.

sion of oxygen exchange between the atmosphere and the water due to an ice cover, sedimentary and water column oxygen demands, and insufficient underwater light energy for photosynthetic oxygen production. Lake ice cover characteristics, e.g., latest ice formation dates and duration of ice covers, are therefore essential to water quality and ecology of ice-covered lakes. Ice thickness in a lake affects the safety of snowmobiles and ice fishermen. Long-term observations of ice covers in cold regions are fairly sparse (Adams and Stefan, 1997). Therefore model predictions of ice cover characteristics of lakes in the contiguous U.S. as a function of latitude, elevation and climate conditions are valuable. For a projected $2 \times CO_2$ climate scenario lake ice characteristics may change significantly, and projections of these changes can be made by model simulation. Climate scenarios are not predictions or forecasts. They represent possible future atmospheric conditions for exploring implications of climate change. $2 \times CO_2$ climate scenarios represent a possible doubling of atmospheric CO_2 and have been most commonly used for climate change effect studies. If and when a global $2 \times CO_2$ climate may occur is not known due to the many uncertainties that remain. Numerical models relating lake ice-covers to atmospheric parameters were previously developed for three Wisconsin lakes (Vavrus et al., 1996) and an arctic lake (Doran et al., 1996), among others.

In this study a process-based model was applied to 209 locations (weather stations) in the contiguous United States under both past and projected $2 \times CO_2$ climate scenarios. Longitude of the stations ranged from 68°1′W to 124°33′W and latitude from 25°48′N to 48°34′N. Elevations of weather stations above mean sea level ranged from 2 m in coastal areas to 2135 m in mountainous areas (Tucson, AZ). It was assumed that lakes studied have the same elevations as the weather stations used. In this paper we present results obtained with a model that simulates the formation, evolution and decay of ice covers on lakes and the associated vertical water temperature profiles using daily weather data as input. The model was calibrated and validated against data from Minnesota and Wisconsin lakes (Fang and Stefan, 1994, 1996a; Fang et al., 1996; Stefan and Fang, 1995, 1997). Coefficients in the model were derived from extensive data (over 5000 water temperature measurements over 48 'lake years', and 128 ice/snow measurements over 8 years) from Minnesota and Wisconsin lakes. This process-oriented, deterministic model can therefore be applied without further calibration (Stefan and Fang, 1997).

To study the response of lakes to climate change on a continental scale, we chose 27 types of lakes (Table 1) and investigated what effects the climate in 209 different locations of the country might have on them. In many locations these lakes simulated are hypothetical lakes. However, the 'systematic' approach of investigating the same lake types at all locations gives a good picture of how different lake types may behave in different parts of the country, especially under a $2 \times CO_2$ climate scenario for which there are no lake data. Measurements in 'real'

Table 1
Morphometric characteristics of 27 lake types used in the continental-scale simulations

Maximum depth	Surface area, A_S	Eutrophic ($z_S = 1.2$ m)	Mesotrophic ($z_S = 2.5$ m)	Oligotrophic ($z_S = 4.5$ m)	Geometry ratio $A_S^{0.25}/H_{MAX}$
Shallow, $H_{MAX} = 4.0$ m	Small (0.2 km^2)	Lake 1	Lake 2	Lake 3	5.3
	Medium (1.7 km^2)	Lake 4	Lake 5	Lake 6	9.0
	Large (10.0 km^2)	Lake 7	Lake 8	Lake 9	14.1
Medium-depth, $H_{MAX} = 13.0$ m	Small (0.2 km^2)	Lake 10	Lake 11	Lake 12	1.6
	Medium (1.7 km^2)	Lake 13	Lake 14	Lake 15	2.8
	Large (10.0 km^2)	Lake 16	Lake 17	Lake 18	4.3
Deep, $H_{MAX} = 24.0$ m	Small (0.2 km^2)	Lake 19	Lake 20	Lake 21	0.9
	Medium (1.7 km^2)	Lake 22	Lake 23	Lake 24	1.5
	Large (10.0 km^2)	Lake 25	Lake 26	Lake 27	2.3

lakes found in different parts of the country under different climate conditions are of great value, but it may be uncertain how the observed results can be transferred from one 'real' lake to another. For these reasons the study of 'generic' lake types is of value and an illustrative supplement to the study of individual real lakes. This paper summarizes past and potential future climate change effects on lakes, especially small lakes with surface areas up to 10 km^2 and depths up to 24 m in the northern cold regions of the contiguous United States.

To study the effects of climate change, projected changes in climate conditions were obtained from the output of the Canadian Climate Center Global Circulation Model (CCC GCM) for a doubling of atmospheric CO_2. This Canadian model was chosen because it couples oceanic processes with atmospheric conditions, has a finer spatial resolution than most other GCM's, full diurnal/annual cycles and snowfall. It is therefore well suited for cold regions. The monthly increments or ratios of weather parameter values between the $1 \times CO_2$ and $2 \times CO_2$ climate scenarios were applied to measured past climate conditions from 1961 to 1979 following a protocol proposed by the U.S. Environmental Protection Agency (Smith and Tirpak, 1989). Results on winter covers of lakes in the contiguous U.S. are given herein for both the past (1961–1979) and the projected $2 \times CO_2$ climate scenarios. Differences of ice cover characteristics between projected and past climate conditions are provided on separate graphs and maps. By interpolation the dependence or sensitivity of ice cover characteristics to climate conditions can be quantified for many small lakes in the contiguous U.S.

2. Ice cover simulation model and model validation

The snow and ice thickness models were originally developed by Gu and Stefan (1990) but have been used with some modifications (Stefan and Fang, 1997; Fang and Stefan, 1996b). To make projections of ice cover characteristics for lakes in the contiguous U.S., a new, process descriptive algorithm, which replaces the previous empirical and lake size dependent criteria for the date of ice formation, was incorporated in the model (Fang et al., 1996). The new algorithm uses a full heat budget equation to estimate surface cooling, quantifies the effect of forced convective (wind) mixing and includes the latent heat removed by ice formation. The algorithm has a fine (0.02 m) spatial (vertical) resolution near the water surface where temperature gradients before freeze-over are the greatest.

The winter ice cover model is associated with a deterministic, one-dimensional (vertical direction) water temperature model (Stefan et al., 1994, 1998; Stefan and Fang, 1995). During the ice cover period, the model simulates ice thicknesses and sediment temperature profiles (by the heat conduction equation) first, then determines the heat source/sink term for each water layer, and finally solves the heat transfer equation to obtain vertical water temperature profiles below the ice. The model uses a stacked layer system, the layers consisting of lake sediments, water, ice cover and snow cover. At the air/snow interface (or air/ice interface if snow is absent), the net heat flux from the atmosphere into or out of the snow/ice cover is calculated. Contributions are made by solar radiation, evaporation and convection. Snow thickness is determined from snow accumulation, followed by compaction and melting of snow by surface heat input (convection, rainfall, solar radiation) and melting within the snow layer due to internal absorption of short wave radiation, and transformation of wetted snow to ice when cracks in the ice cover allow water to spill onto the ice surface (Fang and Stefan, 1996b). In the model ice growth occurs from the ice/water interface downward and from the ice surface upward (Fang and Stefan, 1996b). Ice decay occurs at the snow/ice interface, ice/water interface, and within the ice layer. The complete set of equations used has been summarized by Fang and Stefan (1994, 1996b).

Measured ice thicknesses, snow depths and water temperatures from Ryan Lake, Minnesota (from 1989 to 1995), Thrush Lake, Minnesota (from 1986 to 1991) and Little Rock Lake, Wisconsin (from 1983 to 1991) were used for model validation (Fang and Stefan, 1996a). Standard errors between simulated and measured values were 0.07 m for snow depths and 0.12 m for ice thicknesses for long-term simulations (128 ice/snow measurements over 8 years) in

Thrush Lake and Little Rock Lake. Average standard error between simulated and measured water temperatures during the ice cover period was 0.5°C for these two lakes. Predicted freeze-over dates were compared with observations in nine Minnesota lakes for multiple (1 to 36) years. The difference between the simulated and observed ice formation dates was less than 6 days for all lakes studied (Fang et al., 1996).

Recently Adams and Stefan (1997) assembled additional data of ice cover characteristics in several northern lakes. The physical characteristics of these lakes are summarized in Table 2a. Observed and simulated ice cover characteristics of these lakes are given in Table 2b. Parameters in Table 2b include mean ice-out dates, standard deviations of the mean ice-out dates, mean ice-in dates, standard deviations of the mean ice-in dates, duration of ice cover on lakes, and maximum ice thicknesses. Observed data are from periods of 9 to 140 years. Simulations by

the year-round MINLAKE96 model show good agreement with observations (Table 2b).

3. Model input for continental-scale simulations

The required model input consists of geometric and trophic-state lake characteristics, daily weather data, and initial conditions for vertical water and sediment temperature profiles. The climate and lake characteristics may vary from site to site over the contiguous U.S., but since the model is *process-oriented* the model predictions account for these differences (Fang and Stefan, 1996c). Initial conditions for continental-scale simulations in small lakes have a geographic dependence (Fang and Stefan, 1996c, 1998).

3.1. Generic lake types

'Generic' lake types with surface areas up to 10 km^2 and depths up to 24 m were investigated. The

Table 2

(a) Summary of physical lake characteristics (Adams and Stefan, 1997)

Lake Name	Location (State)	Latitude	Longitude	Surface area (km^2)	Maximum depth (m)	Period of data (year)
Moosehead Lake	Maine	45°45′N	69°45′W	331.0	75.0	1848–1988
Allequash Lake	Wisconsin	46°02′N	89°37′W	1.684	8.0	1981–1990
Big Muskellunge Lake	Wisconsin	46°01′N	89°37′W	3.963	21.3	1981–1990
Crystal Bog	Wisconsin	46°00′N	89°36′W	0.005	2.5	1981–1990
Crystal Lake	Wisconsin	46°00′N	89°37′W	0.367	20.4	1981–1990
Sparkling Lake	Wisconsin	46°00′N	89°42′W	0.640	20.0	1981–1990
Trout Bog	Wisconsin	46°02′N	89°41′W	0.011	7.9	1981–1990
Trout Lake	Wisconsin	46°02′N	89°40′W	16.08	35.7	1981–1990
ELA Lake 239	Ontario	49°40′N	93°44′W	0.560	30.4	1969–1995

(b) Observed and simulated ice cover characteristics of lakes in cold regions (Adams and Stefan, 1997)

Lake name	Mean ice-out date (Julian day)	Standard deviation of ice-out date	Mean ice-in date (Julian day)	Standard deviation of ice-in date	Duration of ice cover (days)	Maximum ice thickness (m)
Moosehead Lake	129 (109)[a]	8 (8)[a]	–	–	–	–
Allequash Lake	110 (105)	7 (9)	329 (331)[a]	9 (8)[a]	149 (143)[a]	0.68 (0.70)[a]
Big Muskellung Lake	110 (105)	7 (9)	328 (335)	14 (8)	143 (133)	0.75 (0.70)
Crystal Bog	109 (105)	7 (9)	320 (328)	7 (8)	156 (147)	0.64 (0.70)
Crystal Lake	111 (105)	8 (9)	335 (335)	7 (8)	142 (133)	0.68 (0.70)
Sparkling Lake	111 (105)	8 (9)	337 (335)	5 (8)	141 (133)	0.70 (0.70)
Trout Bog	112 (105)	7 (9)	322 (331)	5 (8)	157 (143)	0.59 (0.70)
Trout Lake	116 (105)	7 (9)	346 (335)	8 (8)	138 (133)	0.66 (0.70)
ELA Lake 239	120 (120)	7 (8)	321 (323)	6 (7)	165 (155)	–

[a] Numbers outside and inside of parentheses are observed and simulated values, respectively.

lake geometry (bathymetry) is characterized by (a) a surface area A_S, (b) a maximum depth H_{MAX}, and (c) a function $A(z)/A_S$ given as

$$\frac{A(z)}{A_S} = a\exp\left(b\frac{z}{H_{MAX}}\right) + c \tag{1}$$

which characterizes the shape of the lake basin as a function of depth z. Coefficients (a, b, and c) in Eq. (1) were chosen by regression analysis from data for 122 Minnesota lakes (Hondzo and Stefan, 1993).

Lake surface areas A_S chosen are 0.2, 1.7 and 10.0 km^2 for small, medium and large lakes, respectively (Table 1). Maximum depths H_{MAX} chosen are 4, 13 and 24 m for shallow, medium-depth and deep lakes, respectively (Table 1). These numerical specifications are arbitrary but cover the range of lakes in Minnesota (Hondzo and Stefan, 1993). With these six numbers, one obtains nine lake types ranging from relatively large and shallow lakes to relatively small and deep lakes. The likelihood of a strong or weak stratification in a lake can be related to the lake geometry ratio $A_S^{0.25}/H_{MAX}$ (Gorham and Boyce, 1989). The above nine types of lakes cover geometry ratios from 0.9 to 14.1 (see Table 1). Polymictic lakes have the high numbers, while strongly stratified lakes occur at the lowest numbers. The transition occurs between 3 and 5. Hence the full range of stratification behavior is included in the 27 lake types selected for study.

Secchi depth, a common limnological measure of lake transparency obtained by lowering a 20 cm diameter disc into a lake and recording the depth at which it disappears from view, was used to represent both trophic state and radiation attenuation in a lake. Secchi depths of 1.2, 2.5, and 4.5 m for eutrophic, mesotrophic, and oligotrophic lakes were selected, respectively. Therefore the 27 'generic' lake types (Table 1) were characterized by combining three different lake surface areas, three lake maximum depths and three Secchi depths ($3 \times 3 \times 3$).

3.2. Past and projected $2 \times CO_2$ climate scenarios

Meteorological conditions drive water temperatures, ice cover formation, ice growth and ice melting on a lake. Weather data are model inputs, and consist of daily air temperature, dew point tempera-

ture, wind speed, solar radiation, total cloud cover, and precipitation (both rainfall and snowfall). Weather data were obtained from the National Climatic Data Center (CDSAMSON). Weather data used to describe past climate conditions were records from 1961 to 1979. Distribution of the 209 weather stations used is shown in Fig. 1 (dots on the top map). Longitude of the stations ranged from 68°1′W to 124°33′W and latitude from 25°48′N to 48°34′N. Elevations of weather stations above mean sea level (bottom map) ranged from 2 m in coastal areas to 2135 m in mountainous areas (Tucson, AZ). The weather stations used are typically in or near towns, and the lake simulations made are therefore not representative of alpine conditions. The lakes simulated have the same elevations as the weather stations used.

The output of the Canadian Climate Center Second-Generation General Circulation Model (CCC GCM) (McFarlane et al., 1992; Boer et al., 1992) was used to specify the monthly increments or ratios in climatic parameter values due to a doubling of atmospheric CO_2. The second generation CCC GCM includes higher spatial resolution $3.75° \times 3.75°$ than previous models, and full diurnal/annual cycles. The CCC GCM grid center points within or near the contiguous U.S. are given as crosses on the top map of Fig. 1. Monthly climate parameter increments or ratios obtained from the CCC GCM were applied to past climate conditions (1961 to 1979) to generate the projected $2 \times CO_2$ climate scenario following a protocol proposed by the U.S. Environmental Protection Agency (Smith and Tirpak, 1989). Monthly increments or ratios from the grid center point closest to a weather station were used for that station. Therefore the same mean monthly adjustments could be used for two or more stations if they are all close to a particular grid center point.

The mean annual air temperatures under past and projected $2 \times CO_2$ climate conditions interpolated from 209 weather stations are shown in Fig. 2. They strongly depend on latitude and altitude and weakly on longitude of the stations. The difference of the mean annual air temperatures from the northern border to the southern border of the U.S. is about 18°C under past climate conditions, and is projected to be about 15°C under the $2 \times CO_2$ climatic scenario. This is one reason why ice cover characteristics in
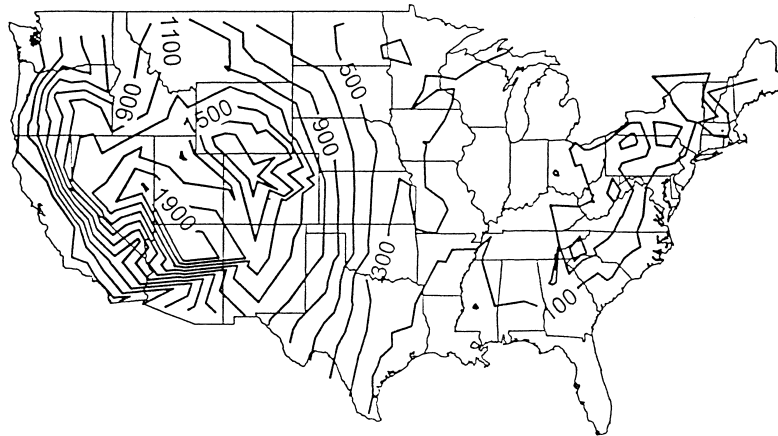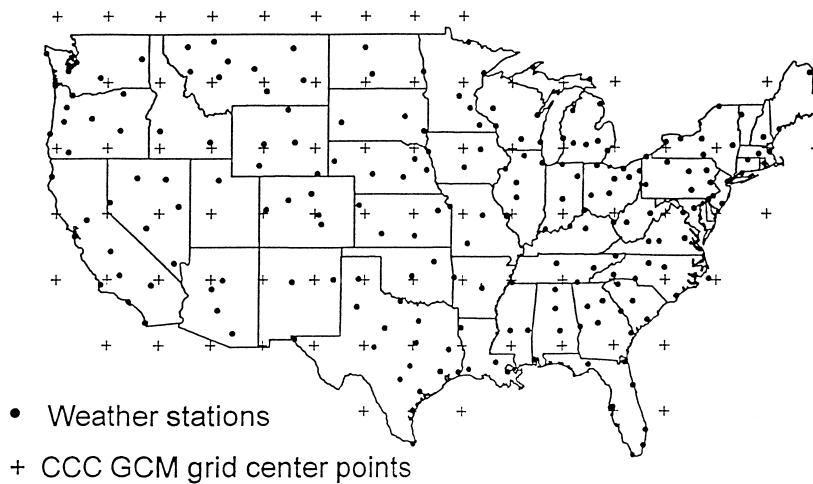
Fig. 1. Locations of weather stations (dots) and grid center points (crosses) of the $2 \times CO_2$ Canadian Climate Center Global Circulation Model (CCC GCM) used in the continental-scale simulations (top map). Elevations (m) of weather stations above mean sea level (bottom map).

lakes of the contiguous U.S. depend strongly on geographic location, especially latitude. The mean annual air temperatures are projected to increase by 2.5°C to 6.5°C (bottom map of Fig. 2). Increases of air temperature are greater in northern latitudes than in southern latitudes. Increases are not uniform throughout a year. For example, the average increases of air temperature during January, range from 10°C in the north to 2°C in the south. The average increases of air temperature for the periods from April to June and July to December range from

3 to °C, and from 2.5 to 6°C (Fang and Stefan, 1996c), respectively, i.e., they are smaller than for January. As a general measure of winter severity, cumulative degree days of freezing are often used. Maps giving degree days of freezing for past and $2 \times CO_2$ climate scenarios as well as difference between the two are given in Fig. 3. Local maximum and minimum values of degree days of freezing for winter periods from 1961 to 1979 ranged from 1712 to 0 and 1003 to 0 under past and projected climate scenarios, respectively. The maximum degree days
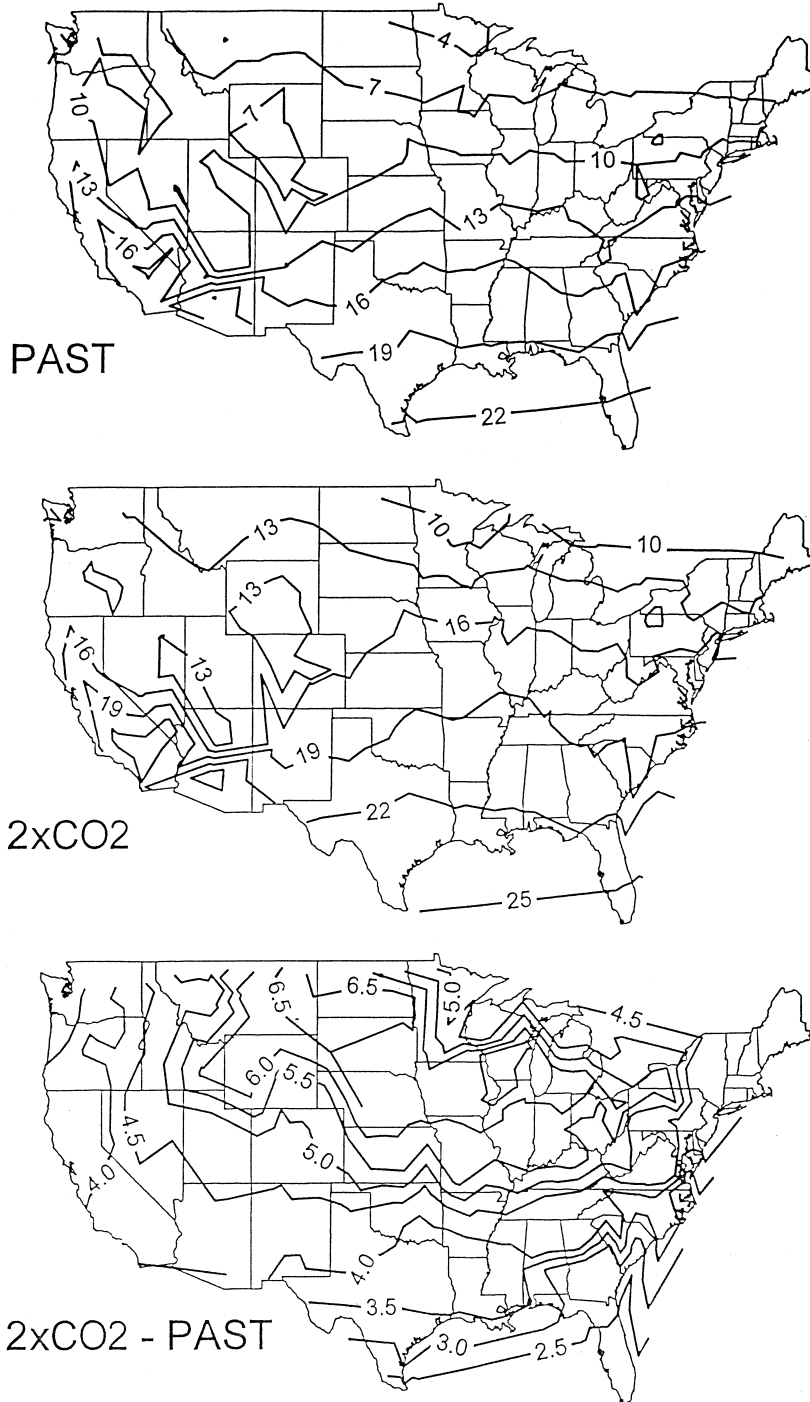
Fig. 2. Mean annual air temperatures (°C) under past (1961–1979) (top) and projected $2 \times CO_2$ (middle) climate conditions; differences between projected and past climate scenarios (bottom).

Fig. 3. Degree (°C) days below freezing under past (1961–1979) (top) and projected $2 \times CO_2$ (middle) climate conditions; differences between projected and past climate scenarios (bottom).
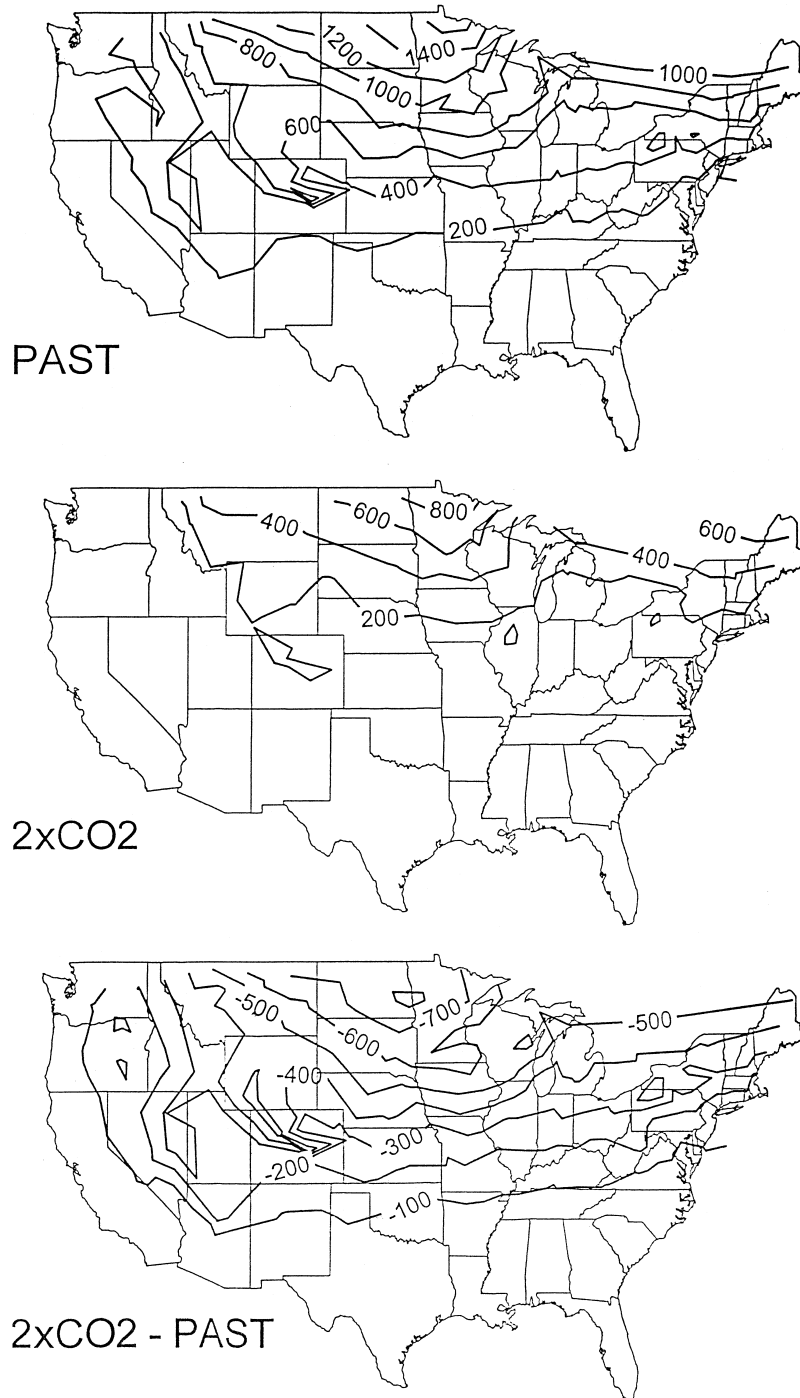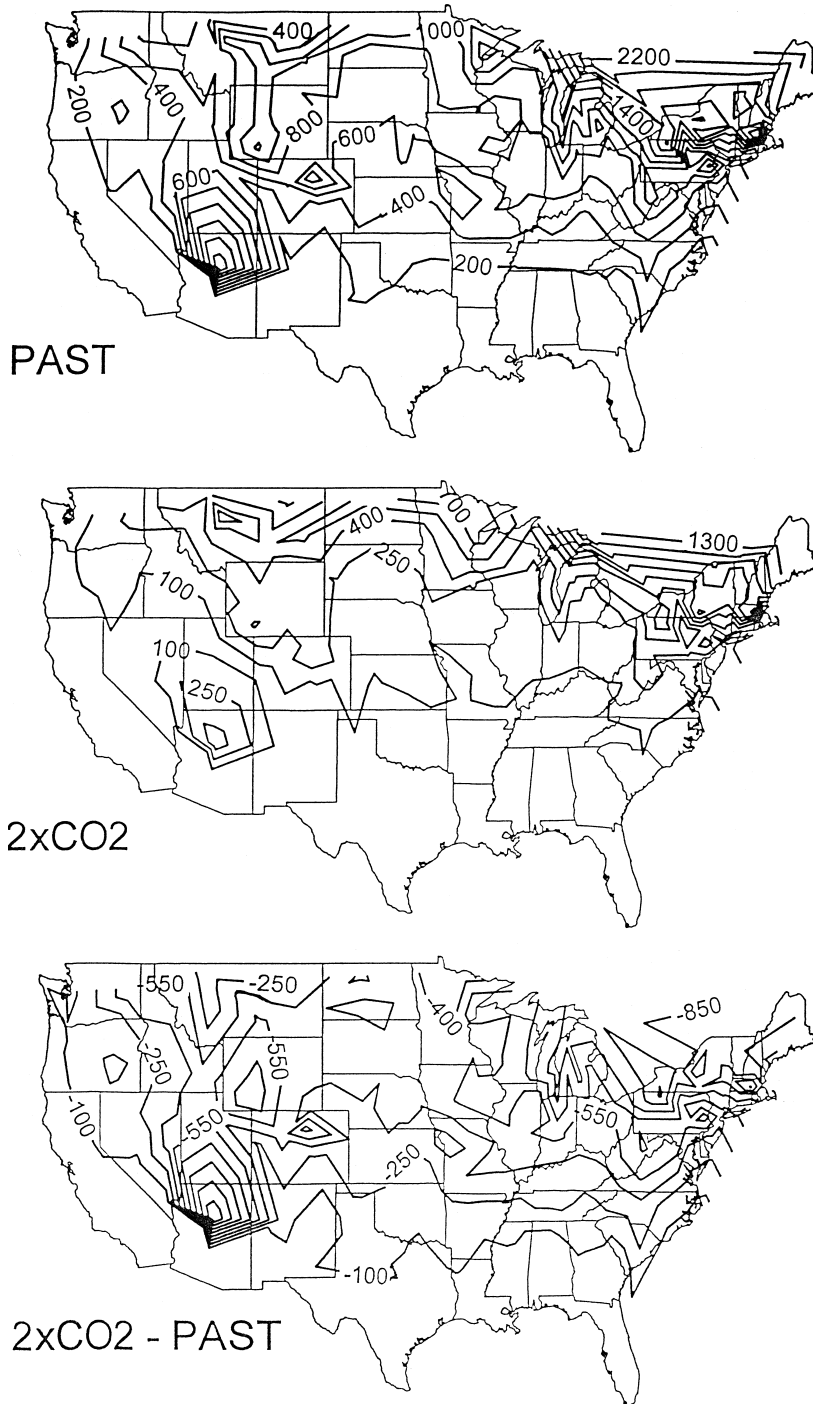
Fig. 4. Average annual snowfall (mm) under past (1961–1979) (top) and projected $2 \times CO_2$ (middle) climate conditions; differences between projected and past climate scenarios (bottom).

of freezing occur near Int. Falls, MN, for both climate scenarios. The differences between projected and past climate ranges from -828 (near Bismarck, ND) to 0. The average degree days of freezing at Rock Springs, WY, are 1004 and 362 for past and projected climate scenarios, respectively.

The precipitation, i.e., snowfall during the winter, is another climate parameter which influences winter ice covers in lakes. Average annual snowfall (mm) under past and the projected $2 \times CO_2$ climate conditions shows strong dependence on latitude (Fig. 4). Snowfall does occur at southern latitudes (Fang and Stefan, 1996c), but has little correlation with ice formation on a lake (water temperatures in southern lakes are still too high to allow ice formation). The CCC GCM output specifies the precipitation change as the ratio of precipitation under the projected $2 \times CO_2$ climate to that under past climate (1961 to 1979). Precipitation changes are projected by the CCC GCM for both rainfall and snowfall. When the daily air temperature was below the freezing temperature (0°C) precipitation was treated as snowfall. Average annual snowfall is projected to decrease by amounts ranging from 100 to 1000 mm depending on geographic location (bottom map of Fig. 4).

4. Modeling procedure and parameterization for continental-scale simulations

The year-round lake water temperature model MINLAKE96 was run in a continuous mode and in daily timesteps with weather data input for a 19-year period (1961–1979) and for 27 lake types. The simulations started with 1 January 1961, using geographically dependent initial conditions for water and sediment temperatures Fang and Stefan, 1996c, 1998). The model coefficients and parameters were kept constant over the simulation period. Lake geometry (surface area, maximum depth, bathymetry), summer Secchi depth and weather data were the model input. Simulations were carried out for 209 locations over the contiguous United States. Simulations were then repeated with the projected $2 \times CO_2$ (CCC GCM) climate scenario at the same stations.

As an example of model output, Fig. 5 shows simulated ice thickness (m) for Lake 10 (Table 1) under 1962–1963 and projected $2 \times CO_2$ climate conditions near Des Moines, Iowa. For lakes in the cold regions eight ice cover characteristics (Table 3) were extracted for every winter period. For illustration, values of these parameters for the lake in Fig. 5
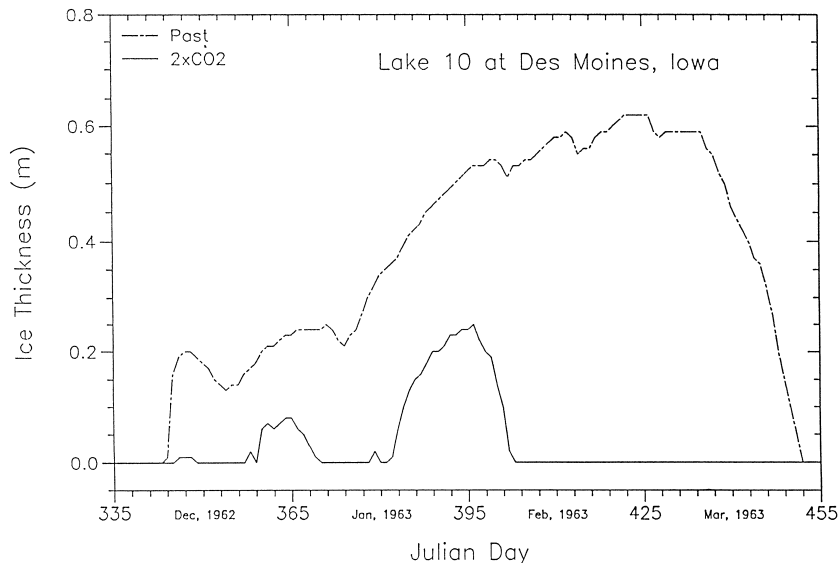

Fig. 5. Simulated ice thicknesses (m) in Lake 10 under 1962–1963 and projected $2 \times CO_2$ climate conditions at Des Moines, Iowa.

Table 3
Parameters used to define long-term winter ice-cover characteristics

Parameter	Description	Past[a]	$2 \times CO_2^a$
Earliest ice-in date	First day with ice cover in fall, but ice may melt out $\{t_{ei}\}$	344	346
Latest ice-in date	Last day with open water in fall; followed by ice growth and winter ice cover	344	382
Earliest ice-out date	First day without ice cover in spring, but ice cover may form again	451	402
Latest ice-out date	Last day with ice cover in spring, followed by open water season $\{t_{io}\}$	451	402
Duration of ice cover	Total number of cumulative days with lake ice cover $\{D_{ice}\}$	108	36
Total period of ice cover	Days between earliest ice-in and latest ice-out dates $\{t_{io} - t_{ei}\}$	108	57
Continuous ice cover ratio	Duration of ice cover divided by total period of ice cover $\{D_{ice}/(t_{io} - t_{ei})\}$	1.0	0.63
Maximum ice thickness (m)	Maximum ice thickness over winter ice cover period $\{Max[\delta_{ice}, t = 1,365]\}$	0.62	0.25

[a] Values are for Fig. 5 (Lake 10 at Des Moines, IA).

are given in the last two columns of Table 3. The selected characteristics have ecological significance, e.g., the survival and growth of fishes. Since the main objective of the investigation was to identify trends/changes in ice cover characteristics in response to climate change, and not extreme values which may occur over the simulation period, only the means and the standard deviations of the 18 annual values of the simulated parameters are reported herein. Results for the first year of simulations (1961) were not counted to eliminate possible carry-over from the initial conditions.

Characteristic lake ice cover values were plotted against lake surface area, maximum lake depth, and Secchi depth. The surface area, A_S, and maximum depth, H_{MAX}, were combined in a lake geometry ratio $[A_S^{0.25}/H_{MAX}, (m^{-0.5})]$ which was previously shown (Gorham and Boyce, 1989; Stefan et al., 1993) to be a good relative measure of a lake's susceptibility to stratify; Secchi depth z_S was retained as a measure of lake transparency (radiation attenuation) and trophic state. The 27 lake types are more or less uniformly distributed on plots using lake geometry ratio and Secchi depth as axes. Since these types of plots were introduced in a paper by Stefan and Fang (1997), explanation will not be repeated here. Plots were made for five geographic locations (Fang and Stefan, 1996c), i.e., Duluth, MN (92°11′W, 46°50′N, elevation 432 m), Minneapolis, MN (93°13′W, 44°53′N, elevation 255 m), Boulder, CO (105°15′W, 40°01′N, elevation 1632 m), Kansas City, MS (94°43′W, 39°18′N, elevation 315 m), and Charleston, WV (81°36′W, 38°22′N, elevation 290 m). If a dependence of an ice cover characteristic on lake geometry ratio and Secchi depth exists, it was

usually similar from one location to another (Fang and Stefan, 1996c).

By interpolation of the values simulated at 209 locations, isolines of ice cover characteristics were obtained and plotted on a U.S. base map with state boundaries (Figs. 6–11). Dependent on the variation of an ice cover characteristic with the lake geometry ratio and Secchi depth, U.S. maps were prepared for one or several lake types to show dependence of that characteristic on geographic location in the entire U.S. Isolines simulated for the past climate conditions are given at the top, values simulated for the projected $2 \times CO_2$ climate scenario are given in the middle, and difference between ice cover characteristics simulated under the projected and the past climate conditions at the bottom of Figs. 6–10. These figures therefore provide a good idea of the projected effect of climate change on several ice cover characteristics. Each figure will be discussed in more detail in Section 5.

5. Projections of lake ice cover characteristics under different climate conditions

5.1. Frequency of ice cover formation on lakes

The number of years with ice cover (simulated) divided by the total number of years simulated, i.e., 18 years (1962–1979), is given in Fig. 6 as an average for all 27 lake types investigated. A ratio less then 1.0 indicates that an ice cover did not form on a lake every year during the simulation period (an ice cover needs to form for only one day to be considered). Under a $2 \times CO_2$ climate scenario the ratio is projected to decrease by a mean value of 0.17
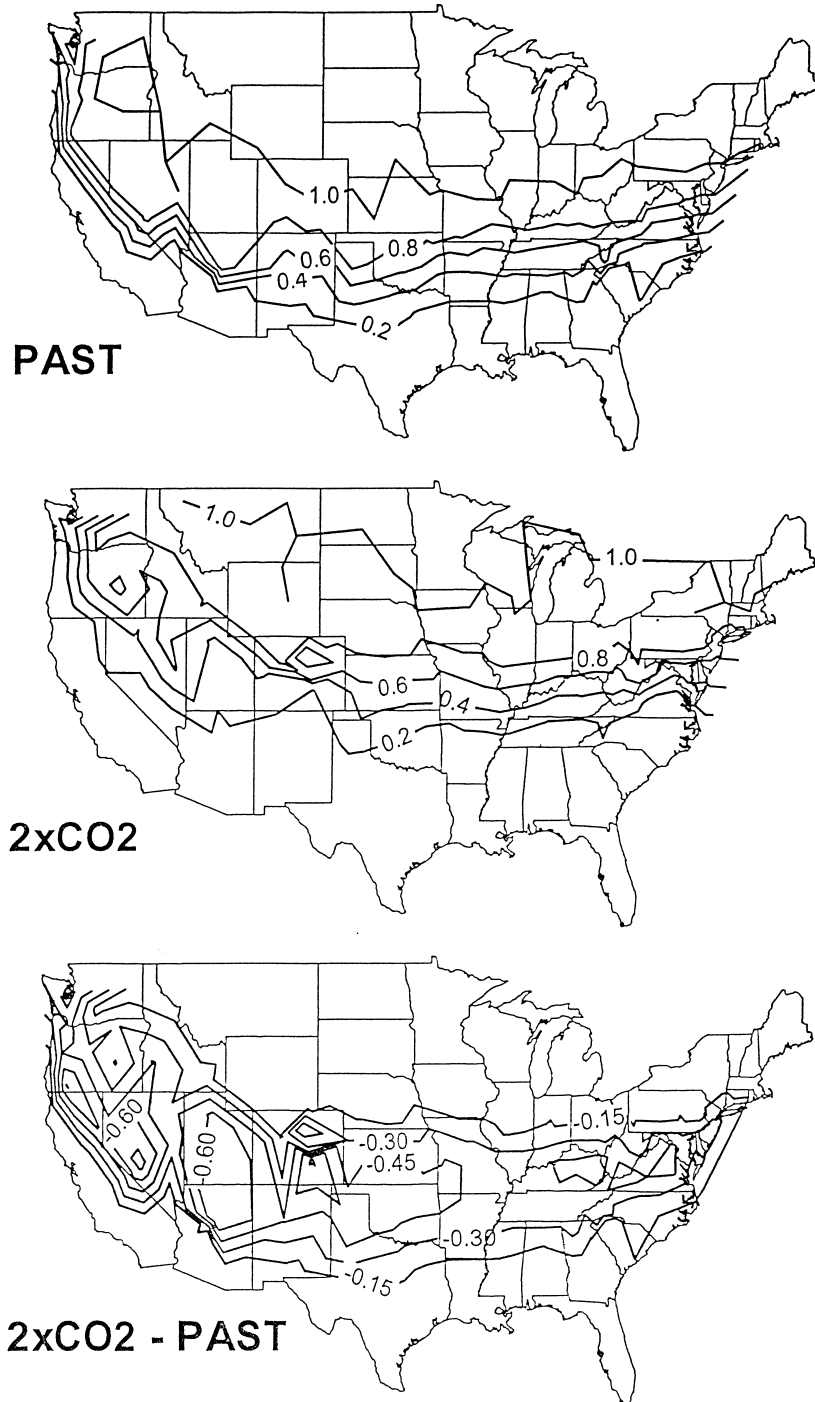
Fig. 6. Ratio of number of years with ice cover on lakes to the 18-year simulation period under past (1962–1979) (top) and projected $2 \times CO_2$ (middle) climate conditions; differences between projected and past climate scenarios (bottom).
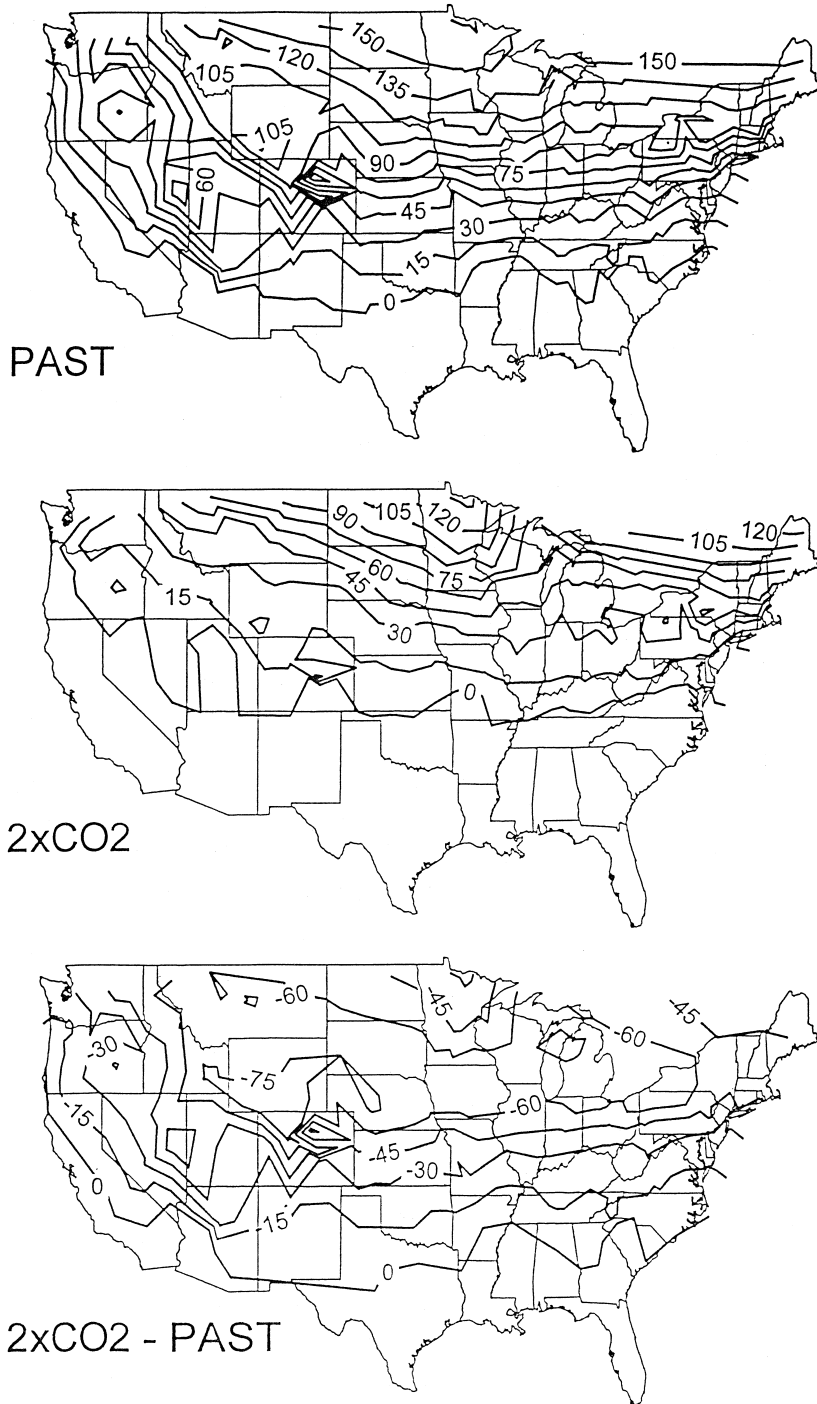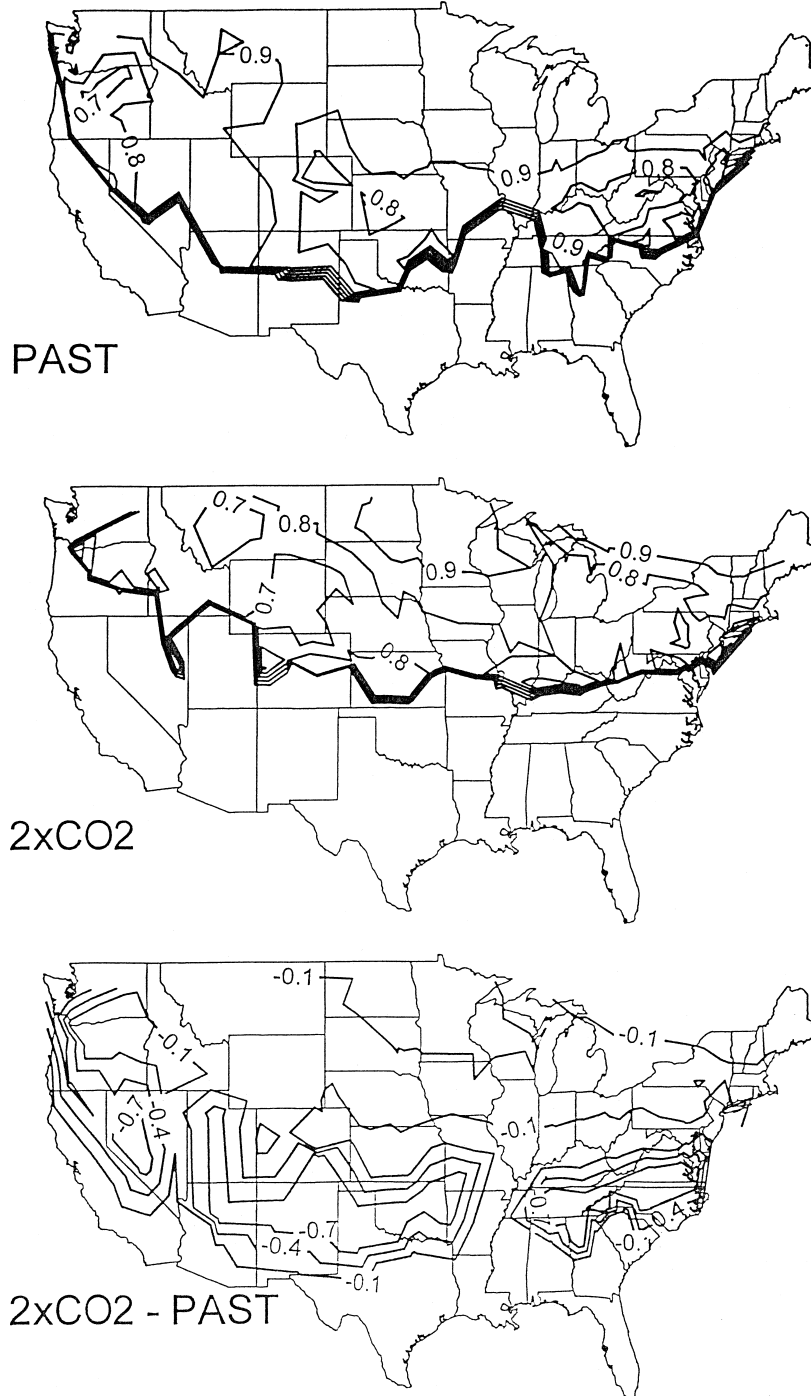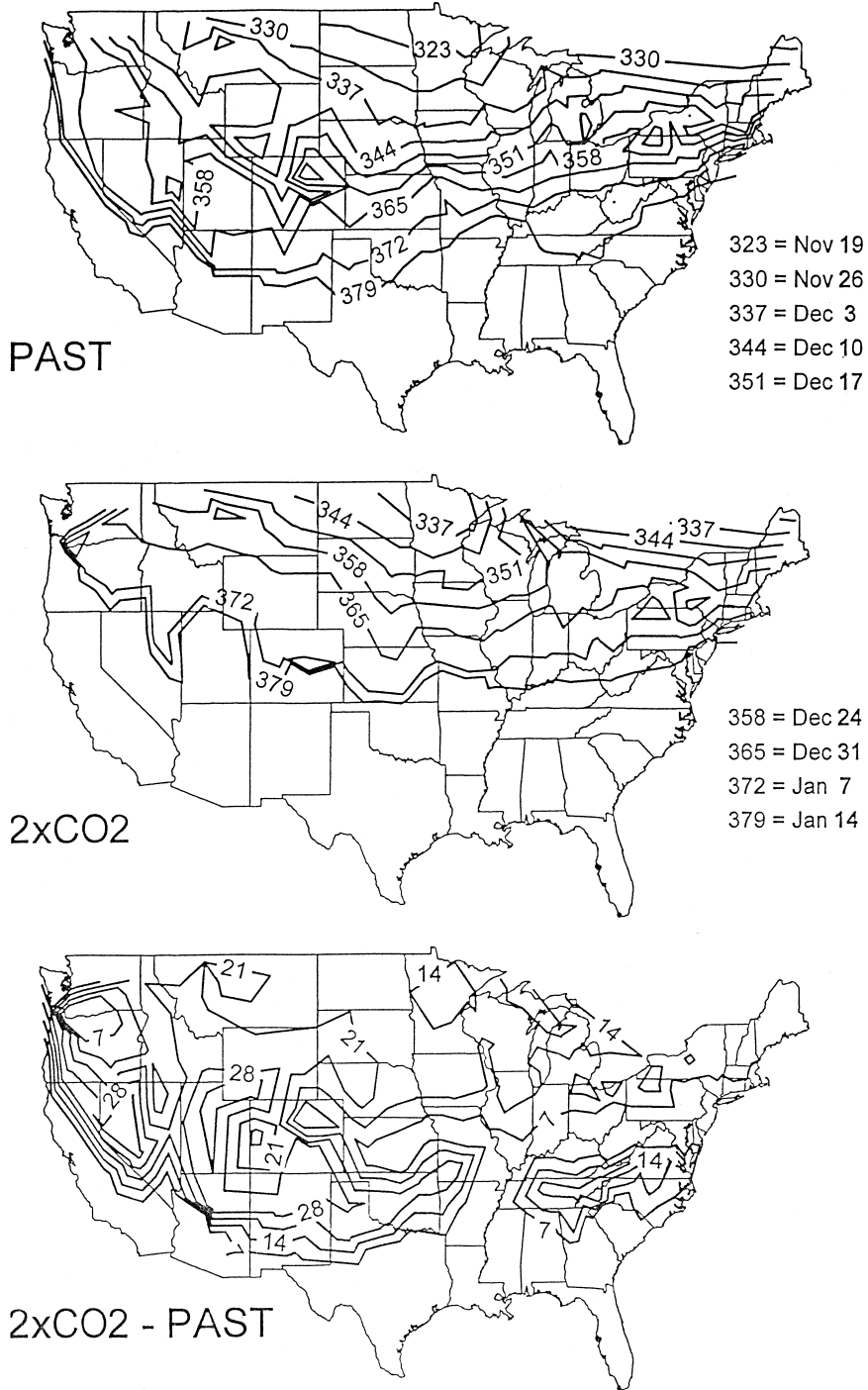
Fig. 7. Simulated annual cumulative days of ice cover on small, medium-depth ($H_{\mathrm{MAX}} = 13$ m) lakes under past (1962–1979) (top) and projected $2 \times CO_2$ (middle) climate conditions; differences between projected and past climate scenarios (bottom).

Fig. 8. Simulated annual continuous ice cover ratio for small, medium-depth (H_{MAX} = 13 m) lakes under past (1962–1979) (top) and projected $2 \times CO_2$ (middle) climate conditions; differences between projected and past climate scenarios (bottom).
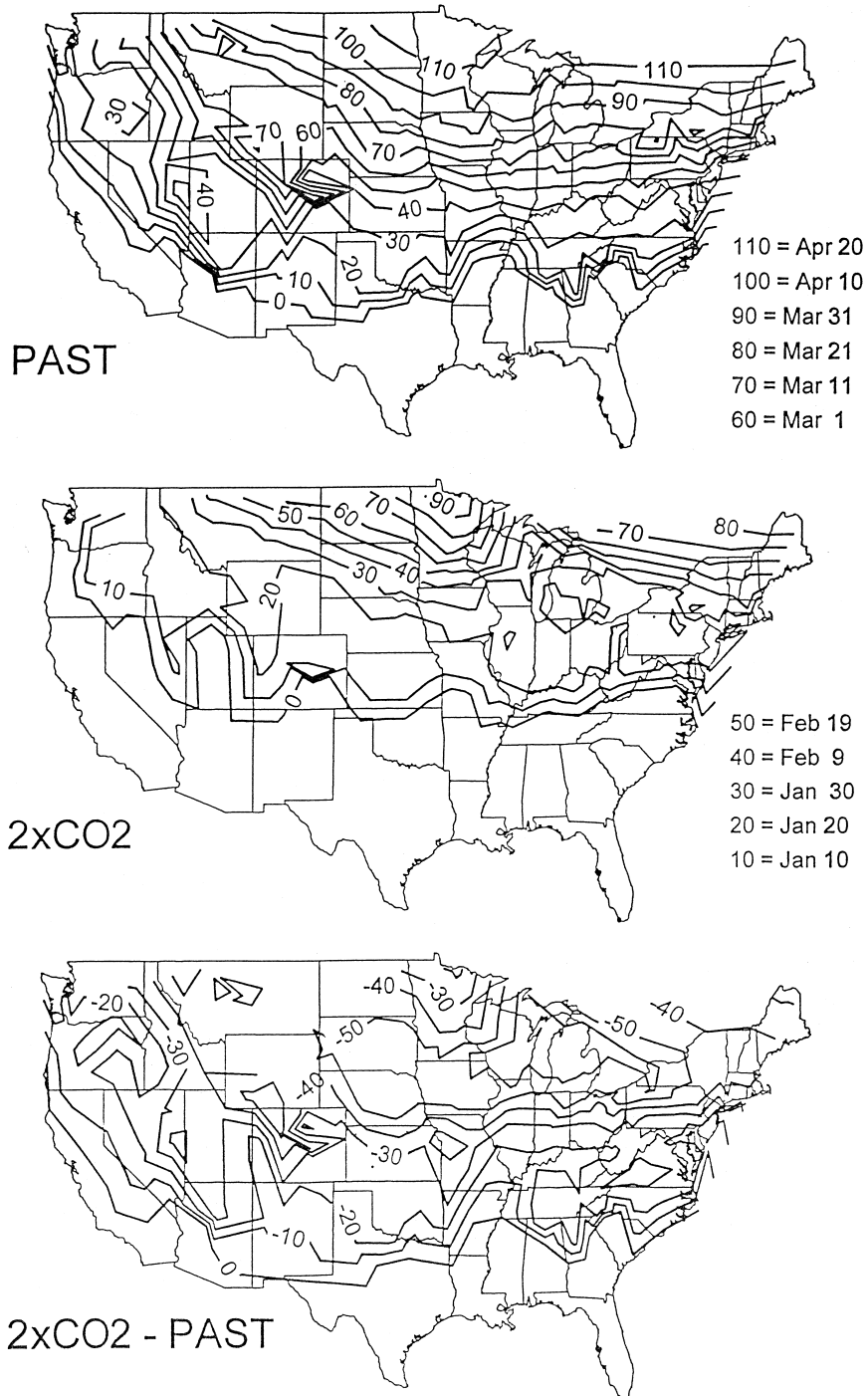
Fig. 9. Simulated latest annual ice-in dates for small, medium-depth (H_{MAX} = 13 m) lakes under past (1962–1979) (top) and projected $2 \times CO_2$ (middle) climate conditions; differences between projected and past climate scenarios (bottom).

Fig. 10. Simulated earliest annual ice-out dates for small lakes under past (1962–1979) (top) and projected $2 \times CO_2$ (middle) climate conditions; differences between projected and past climate scenarios (bottom).

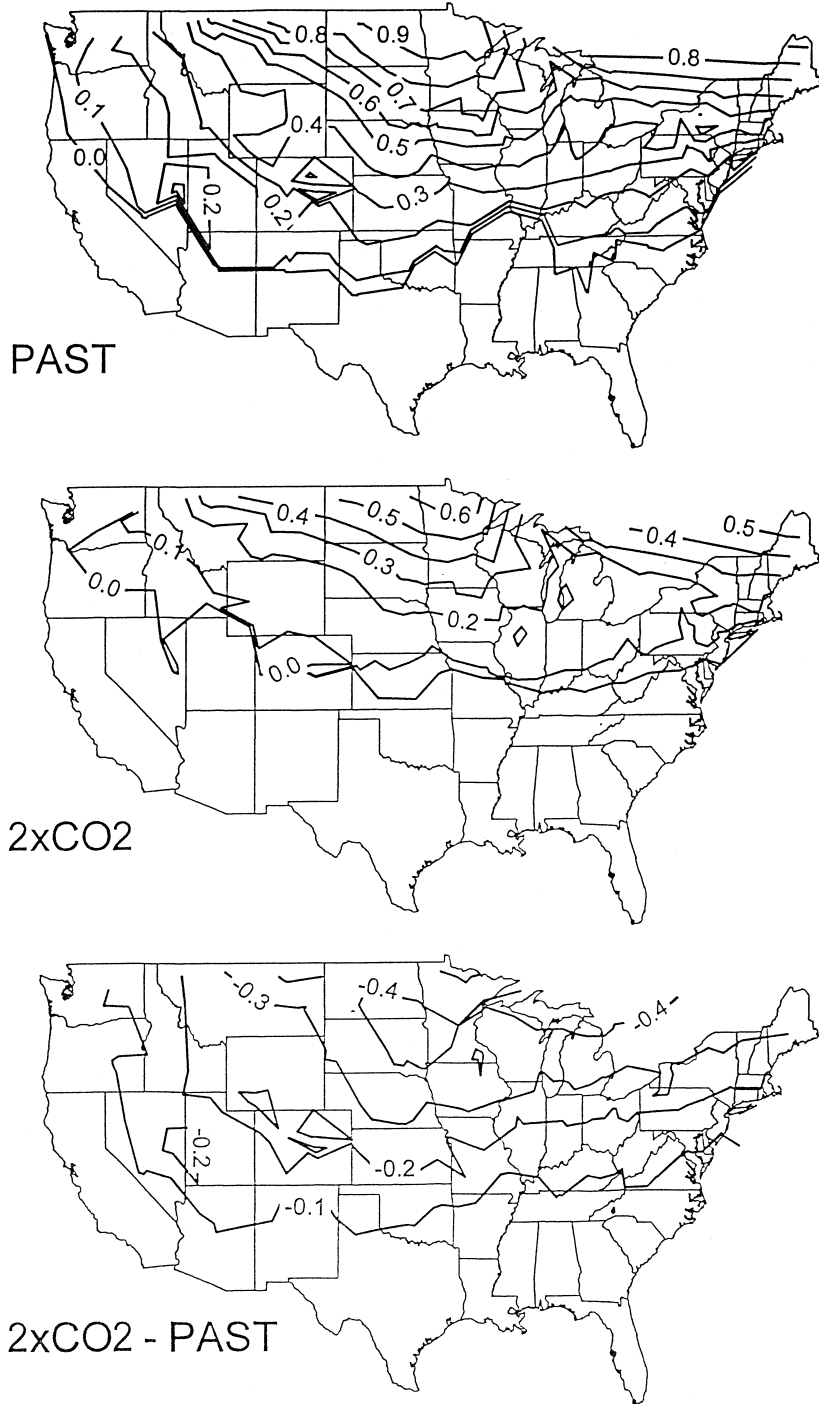Fig. 11. Simulated maximum annual lake ice thicknesses (m) on small lakes under past (1962–1979) (top) and projected $2 \times CO_2$ (middle) climate conditions; differences between projected and past climate scenarios (bottom).

(standard deviation of 0.20) for the contiguous U.S. The local maximum decrease due to climate warming is 0.81 near Tonopah, Nevada. This is about a 15-year change over an 18-year simulation period. Changes due to climate warming occur mainly in a belt which runs from Washington/Oregon, through Kansas/Oklahoma to Virginia (see bottom map of Fig. 6). The number of stations in the contiguous U.S. where ice cover is predicted to form for at least one day on a lake *every year* is projected to *decrease* from 105 (past) to 38 ($2 \times CO_2$). The number of stations where no ice cover is projected to form in any year *increases* from 40 (past) to 59 ($2 \times CO_2$). The boundary between areas with or without ice cover on lakes in *every year* (ratio = 1.0) corresponds closely to the line representing 400 degree (°C) days below freezing under both past and projected climate scenarios (Fig. 3). As the 400 degree days line moves towards a more northern latitude due to climate warming (Fig. 3), so does the 1.0 ratio line. For those geographic locations where the ratio is greater than 0.0 and up to 1.0, simulated ice cover characteristics are shown in Figs. 7–11 as defined in Table 3.

5.2. Duration of ice cover on lakes

The *duration of ice cover* (Fig. 7) is the number of cumulative, not necessarily continuous, days when an ice cover is present on a lake. Lake geometry ratio has only a weak influence and lake trophic status has virtually no influence, but latitude and elevation, i.e., weather conditions, have a strong influence on the length of the ice cover period (Stefan and Fang, 1997; Fang and Stefan, 1996c; Fang et al., 1997; Vavrus et al., 1996). In Fig. 7 the differences in the average duration of lake ice covers over the contiguous U.S. for nine medium-depth (13 m maximum depth) lakes are shown. Duration of ice cover on these medium-depth lakes is about 7 days longer than for shallow lakes, and about 7 days shorter than for deep lakes (Fang and Stefan, 1996c; Fang et al., 1997). Total duration of lake ice cover is presently up to 167 days near the northern border of the contiguous U.S. (International Falls, MN), where it is projected to decrease to 141 days under the CCC

GCM $2 \times CO_2$ climate scenario. Overall the total duration of lake ice cover is projected to shorten by up to 89 days under the warmer $2 \times CO_2$ climate scenario. The maximum reduction occurs in Rock Springs, WY. The highest and lowest local values do not appear explicitly on the maps of Figs. 7–11, and were therefore listed in Table 4 including mean values and standard deviations of local values.

Standard deviations from the mean ice cover duration over the 18-year simulation period are from 6 to 27 days (Fang and Stefan, 1996c; Fang et al., 1997) and depend on geographic location. The larger variations occur in the south. For lakes that have an *ice cover every year* (see Fig. 6) the mean duration of ice cover is predicted to be greater than 45 days under both past and $2 \times CO_2$ climate conditions. Possible ice cover formation (duration $\geqslant 1$ day, Fig. 7) on lakes is projected to move from the northern Texas/southern Oklahoma border under present climate conditions towards the southern boundaries of Kansas and Missouri under the projected $2 \times CO_2$ climate scenario. Ice cover durations and ice thicknesses have traditionally been related to cumulative degree days of freezing. Maps of the contiguous U.S. showing cumulative degree days of freezing for past climate and a $2 \times CO_2$ climate scenario were therefore prepared (Fig. 3) and showed regional patterns and relative changes similar to those in Fig. 7.

5.3. Continuity of ice cover

The *continuous ice cover ratio* (Fig. 8) measures whether an ice cover is continuous or discontinuous. It is calculated as the number of cumulative days with ice cover divided by the total period of ice cover which is defined as the period from first freeze-over to last ice-out (Table 3). A value of 1.0 indicates a continuous ice cover such as shown, for example, for past climate conditions in Fig. 5. A discontinuous ice-cover is one that melts and then forms again at least once in a given winter, e.g., the ice cover under a $2 \times CO_2$ climate scenario in Fig. 5. If the continuous ice cover ratio is small, ice cover may not have a significant impact on lake water quality, e.g., dissolved oxygen concentration, even though the ice cover period is long, because between

Table 4
Means and extremes of simulated ice cover characteristics at 209 locations in the contiguous U.S.

Statistical parameters	Climate scenarios	Latest ice-in date[a] (Julian day)	Earliest ice-out date[b] (Julian day)	Duration of ice-cover[c] (days)	Continuous ice cover ratio[d]	Maximum ice thicknesses[e] (m)
Maximum	Past	389	118	167	1.00	0.967
	$2 \times CO_2$	382	101	141	0.99	0.695
	Difference[f]	40	−67	−89	0.19	−0.444
Minimum	Past	318	9	6	0.65	0.012
	$2 \times CO_2$	39	10	7	0.60	0.032
	Difference[f]	−8	−5	−6	−1.00	−0.012
Mean	Past	357	59	75	0.89	0.343
	$2 \times CO_2$	363	29	38	0.80	0.173
	Difference[f]	15	−37	−45	−0.27	−0.210
Standard deviation from the mean	Past	17	28	44	0.084	0.231
	$2 \times CO_2$	11	17	28	0.087	0.127
	Difference[f]	10	16	22	0.337	0.112

[a] Only for medium-depth lakes (Fig. 9).
[b] For all 27 lake types (Fig. 10).
[c] Only for medium-depth lakes (Fig. 7).
[d] Only for medium-depth lakes (Fig. 8).
[e] For all 27 lake types (Fig. 11).
[f] Difference = $2 \times CO_2$ − Past.

two ice formation dates open water will be reoxygenated by reaeration. Lake trophic status has virtually no influence on the continuous ice cover ratio (Stefan and Fang, 1997). Simulated continuous ice cover ratios were averaged for lakes with the same depth and plotted for all 209 weather stations over the contiguous U.S. Fig. 8 gives an example for medium-depth (H_{MAX} = 13 m) lakes. As to be expected ice covers are more continuous in the north than in the south (Fig. 8), and more continuous in deep lakes than in shallow lakes (Fang and Stefan, 1996c; Fang et al., 1997). The average continuous ice cover ratio did not reach 1.0 even at the northern latitudes in the contiguous U.S. because warm weather conditions follow the first ice formation in some years, melting the ice cover on a lake and causing a second ice formation one or several days later. Differences between projected and past climate conditions affect continuous ice cover ratios only little when lakes have an ice cover every year (e.g., lakes in Minnesota and Wisconsin). Large differences exist in southern latitudes (local maximum decrease of 1.0 near Atlanta, GA, Table 4) where ice

covers will not form any more under the $2 \times CO_2$ climate scenario.

5.4. Ice-in and ice-out dates

The *last* (latest) ice-in date in fall or winter is the date after which the ice cover exists continuously until spring ice-out. Discontinuous ice covers predominantly form at the beginning of winter (see Fig. 5). After continuous ice cover formation no further aeration of the water through the lake surface occurs. Trophic state has little effect on the ice-in-date, but variations in lake depth cause variations of up to 6 days in the mean value of this date (Fang and Stefan, 1996c; Fang et al., 1997). Simulated average dates for the latest ice-in under past and projected $2 \times CO_2$ climate scenarios were plotted as Julian days for medium-depth (H_{MAX} = 13 m) lakes over the contiguous U.S. (Fig. 9). The date for each isoline is also given in Fig. 9, e.g., 19 November is Julian day 323. 'Julian day' is given continuously throughout a winter, e.g., ice formation on 7 January would be

372. There appears to be a good correlation between the frequency of ice formation (Fig. 6) and the latest date of freeze-over (Fig. 9). Lakes with ice cover every year (Fig. 6) have ice formation before 31 December (Julian day 365), while lakes with ice cover in only some years have ice formation after 31 December.

Standard deviations from the mean latest ice-in date vary from 12 days in the north to 21 days in the south (Fang and Stefan, 1996c; Fang et al., 1997), i.e., ice covers are most predictable in the coldest climates. Projected climate change delays ice formation about 14 days from 19 November (past) to 3 December ($2 \times CO_2$) near Duluth, MN (bottom map of Fig. 9). For medium-depth lakes in the entire contiguous U.S., climate change delays ice formation by up to 40 days with a mean value of 15 days and a standard deviation of 10 days (Table 4).

The *first* (earliest) ice-out date is the first date in spring on which the ice cover has disappeared. Trophic state and geometry of a lake have little effect on ice-out date because air temperature and solar radiation are primarily responsible for ice melting. Therefore latitude and altitude are important (Fang and Stefan, 1996c; Fang et al., 1997; Stefan and Fang, 1997). Earliest ice-out dates were averaged over the 27 lake types and plotted for the contiguous U.S. (209 weather stations) in Fig. 10. Standard deviations from the mean latest ice-out date (Fang and Stefan, 1996c; Fang et al., 1997) increase from north to south (about 12 days in Duluth, MN and 27 days in Kansas City, MO). If an ice cover occurs on a lake every year (Fig. 6) it is usually present until at least 9 February (Julian day 40) according to Fig. 10. Fig. 10 (middle) shows that this isoline (Julian day 40) moves towards a more northern latitude after climate warming.

Climate warming forces ice on a lake to melt earlier; differences between projected and past climate scenarios for the earliest ice-out dates are typically 37 days (mean value in Table 4). The local maximum change is 67 days near Green Bay, Wisconsin and Muskegon, Michigan. Ice-out in northern Minnesota (Duluth) will occur around March 21 (Julian day 80) under the projected $2 \times CO_2$ climate scenario, about 30 days earlier than the April 20 (Julian day 110) date under past climate conditions. Winterkill occurs mostly in shallow lakes in early

spring due to oxygen depletion. A shift to earlier ice-out dates will reduce winterkill events.

5.5. Maximum ice thicknesses

The *maximum ice thickness* reached in each year (winter) was averaged over 27 lakes and over the 18-year simulation period and is given in Fig. 11. Variations among lakes of different size, depth, and trophic state are no more than 5% or 0.05 m. The period of ice growth after the climate change is shorter and hence maximum ice thicknesses on lakes are less. Maximum ice thicknesses on lakes are projected to be reduced by up to 0.44 m near Sault Ste. Marie, Michigan, with a mean value of 0.21 m (Table 4) due to climate warming.

6. Summary and conclusions

Projected climate change is expected to change aquatic/hydrologic systems strongly in cold regions. This study is concerned with climate change effects on lakes, especially small lakes with surface areas up to 10 km^2 and depths up to 24 m in the northern cold regions of the contiguous United States. A winter ice and snow cover model associated with a deterministic, one-dimensional water temperature model has been applied to 27 lake types at 209 locations (weather stations) in the contiguous United States. The lake parameters required as model input are surface area, maximum depth, and Secchi depth as a measure of radiation attenuation and trophic state. The model is driven by daily weather data and operates year-round over multiple years. Weather records for the period 1961–1979 were used to represent past climate conditions. The projected climate changes due to a doubling of atmospheric CO_2 were obtained from the output of the Canadian Climate Center Global Circulation Model. To illustrate the effect of projected climate change on winter ice cover characteristics, separate maps were presented for values simulated (a) with inputs of past climate conditions (1962–1979), (b) with inputs of the projected $2 \times CO_2$ climate scenario, and (c) differences of values simulated between projected and past climate conditions. Lake ice cover characteristics presented comprise frequency of occurrence and dura-

tion of ice covers, dates of ice-in and ice-out and maximum ice thicknesses.

Over the contiguous U.S. it is projected that there will be a substantial *decrease* in locations where ice covers will form for at least one day on lakes *every year*. Under the $2 \times CO_2$ climate scenario lake ice covers are projected to form every year only in eastern Montana, North Dakota, Minnesota, Wisconsin, Vermont, New Hampshire and Maine (Fig. 6). Ice covers are more continuous in time in the north than in the south of the contiguous U.S. Under past climate (1961–1979), the duration (cumulative days) of ice cover is up to 165 days near the northern border of the contiguous U.S. (International Falls, MN). The duration of ice covers is projected to shorten by up to 89 days (near Rock Springs, WY); it will shorten by a mean value of 45 days after climate warming. Climate change is projected to delay ice formation by up to 40 days (near Rock Springs, WY). Climate warming forces ice on a lake to melt earlier; differences between projected and past climate scenarios for the earliest ice-out date are up to 67 days in Michigan; the mean value is 37 days for the country. Under a $2 \times CO_2$ climatic scenario, maximum ice thicknesses are projected to be reduced by up to 0.44 m (near Sault Ste. Marie, MI) due to climate warming; the mean reduction is 0.21 m for the contiguous U.S. These changes would eliminate fish winterkill in most shallow lakes, but may endanger snowmobiles and fishermen because of reduced bearing capacity of lake ice.

Acknowledgements

References

Adams, C.E., Stefan, H.G., 1997. Field data on lake ice covers: dependence on lake characteristics and climate. Project Report 405. St. Anthony Falls Laboratory, University of Minnesota, Minneapolis, MN.

Ashton, G.D., 1986. River and Lake Ice Engineering. Water Resources Publications, Littleton, CO, 485 pp.

Boer, G.J., McFarlane, N.A., Lazare, M., 1992. Greenhouse gas-induced climate change simulated with the CCC second-generation general circulation model. J. Climatol. 5 (10).

Doran, P.T., McKay, C.P., Adams, W.P., English, M.C., Wharton, R.A., Meyer, M.A., 1996. Climate forcing and thermal feedback of residual lake-ice covers in the high arctic. Limnol. Oceanogr. 41 (5), 832–838.

Fang, X., Stefan, H.G., 1994. Temperature and dissolved oxygen simulations in a lake with ice cover. Project Report 356. St. Anthony Falls Hydraulic Laboratory, University of Minnesota, Minneapolis, MN.

Fang, X., Stefan, H.G., 1996a. Long-term lake water temperature and ice cover simulations/measurements. Cold Regions Sci. Technol. 24 (3), 289–304.

Fang, X., Stefan, H.G., 1996b. Development and validation of the water quality model MINLAKE96 with winter data. Project Report 390. St. Anthony Falls Laboratory, University of Minnesota, Minneapolis, MN.

Fang, X., Stefan, H.G., 1996c. Projections of potential climate change effects on water temperature, dissolved oxygen and associated fish habitat in small lakes of the contiguous U.S., Vol. I—Effects of past climate conditions. Project Report 393. St. Anthony Falls Laboratory, University of Minnesota, Minneapolis, MN.

Fang, X., Stefan, H.G., 1998. Temperature variability in lake sediments. Water Resour. Res., in press.

Fang, X., Ellis, C.E., Stefan, H.G., 1996. Simulation and observation of ice formation (freeze-over) in a lake. Cold Regions Sci. Technol. 24, 129–145.

Fang, X., Pasapula, R., Stefan, H.G., 1997. Projections of potential climate change effects on water temperature, dissolved oxygen and associated fish habitat in small lakes of the contiguous U.S., Vol. II—Effects of projected future climate conditions. Project Report 403. St. Anthony Falls Laboratory, University of Minnesota, Minneapolis, MN.

Gorham, E., Boyce, F.M., 1989. Influence of lake surface area and depth upon thermal stratification and the depth of the summer thermocline. J. Great Lakes Res. 15, 233–245.

Gu, R., Stefan, H.G., 1990. Year-round temperature simulation of cold climate lakes. Cold Regions Sci. Technol. 18 (2), 147–160.

Hondzo, M., Stefan, H.G., 1993. Regional water temperature characteristics of lakes subjected to climate change. Clim. Change 24, 187–211.

McFarlane, N.A., Boer, G.J., Blanchet, J.P., Lazare, M., 1992. The Canadian Climate Centre second-generation general circulation model and its equilibrium climate. J. Climatol. 5 (10).

Smith, J.B., Tirpak, D., 1989. The potential effects of global climate changes on the United State. Report to Congress, USEPA, EPA-230-05-89-050, 413 pp.

Stefan, H.G., Fang, X., 1995. A methodology to estimate year-round effects of climate change on water temperature, ice and dissolved oxygen characteristics of temperate zone lakes with application to Minnesota. Project Report No. 377. St. Anthony Falls Hydraulic Laboratory, University of Minnesota, Minneapolis, MN 55414.

Stefan, H.G., Fang, X., 1997. Simulated climate change effects on ice and snow covers on lakes in a temperate region. Cold Regions Sci. Technol. 25, 137–152.

Stefan, H.G., Hondzo, M., Fang, X., 1993. Lake water quality modeling for projected future climate scenarios. J. Environ. Qual. 22 (3), 417–431.

Stefan, H.G., Hondzo, M., Fang, X., Rasmussen, A.H., 1994. Year-round water temperature and dissolved oxygen simulation model for lakes with winter ice cover. Project Report No. 355. St. Anthony Falls Hydraulic Laboratory, University of Minnesota, 74 pp.

Stefan, H.G., Fang, X., Hondzo, M., 1998. Simulated climate change effects on year-round water temperatures in temperate zone lakes. Clim. Change, in press.

Vavrus, S.J., Wynne, R.H., Foley, J.A., 1996. Measuring the sensitivity of southern Wisconsin lake ice to climate variations and lake depth using a numerical model. Limnol. Oceanogr. 41 (5), 822–831.